

Banner appropriate to article type will appear here in typeset article

A closure mechanism for screech coupling in rectangular twin jets

Jinah Jeun^{1†}, Gao Jun Wu² and Sanjiva K. Lele³

¹Center for Turbulence Research, Stanford University, Stanford, CA 94305, USA

²Department of Aeronautics and Astronautics, Stanford University, Stanford, CA 94305, USA

³Department of Mechanical Engineering and Department of Aeronautics and Astronautics, Stanford University, Stanford, CA 94305, USA

(Received xx; revised xx; accepted xx)

Twin-jet configuration allows two different scenarios to close the screech feedback. For each jet, there is one loop involving with disturbances which originate in that jet and arrive at its own receptivity point in-phase (self-excitation). The other loop is associated with free-stream acoustic waves that radiate from the other jet, reinforcing the self-excited screech (cross-excitation). In this work, the role of the free-stream acoustic mode and the guided jet mode as a closure mechanism for overexpanded twin rectangular jet screech is explored by identifying eligible points of return for each path, where upstream waves propagating from such a point arrive at the receptivity location with an appropriate phase relation. Screech tones generated by these jets are found to be intermittent with an antisymmetric flapping as a dominant coupling mode at this frequency. Instantaneous phase difference between the twin jets computed by the Hilbert transform suggests that a competition between antisymmetric and symmetric coupling is responsible for the intermittency. To model each component of the screech feedback while ensuring perfect phase-locking, an ensemble average of leading spectral proper orthogonal decomposition modes obtained from several segments of large-eddy simulations data that correspond to periods of invariant phase difference is used after a streamwise wavenumber decomposition. The present analysis shows that most of the identified points of return for the cross-excitation are synchronised with the guided jet mode self-excitation, supporting that it is preferred in closing rectangular twin-jet screech coupling.

Key words:

1. Introduction

Supersonic tactical aircraft on during take-off and landing from an aircraft carrier deck operate at off-design conditions, producing deafening sound from its engine exhausts characterised by three distinctive noise components. Turbulent mixing noise, which is attributed to large-scale coherent structures contained in jet turbulence, dominantly radiates at low aft angles. In addition, the shock train formed due to the non-ideal expansion generates the broadband

† Email address for correspondence: jinahjeun@gmail.com

shock-associated noise and, sometimes, even screech, via the interaction with the Kelvin-Helmholtz (KH) instability waves. Screech is associated with drastic amplification in sound pressure level within a very narrow-banded frequency bin and radiates mostly upstream, causing significant potential structural damage to the airframe.

Powell (1953) first discovered jet screech, and since then, it has drawn a continuous interest from the aeroacoustic community. He first described that screech is an aeroacoustic resonance, involving with interaction between the shock and the KH instability waves, which produces upstream-travelling sound waves. The receptivity at the nozzle lip then excites new downstream-travelling disturbances, and once they sufficiently develop, they generate upstream travelling sound, sustaining the feedback cycle. The feedback cycle involving upstream- and downstream-travelling waves is now a generally accepted scenario, but there are still many unknowns that need to be addressed.

While the detailed mechanisms in each process of screech generation mentioned above are not fully understood, the nature of the upstream-travelling waves has received considerable attention in recent research. In Powell's early work, the feedback due to free-stream acoustic waves propagating outside jets was stressed. Shen and Tam (2002) were the first who proposed that waves closing the screech feedback of the A2 (axisymmetric) and C (helical) modes of round jets could in fact be an intrinsic neutral mode identified by Tam and Hu (1989). However, they still suggested the A1 (axisymmetric) and B (flapping) modes favour the free-stream acoustic mode as a closure mechanism. In more recent years, there have been several studies using experimental and numerical evidence (Edgington-Mitchell et al. 2018; Gojon et al. 2018; Li et al. 2020) that support the guided jet mode as a unified closure mechanism for both axisymmetric modes. Mancinelli et al. (2019) demonstrated that screech frequency prediction based on the jet mode showed enhanced accuracy, compared to the result obtained by the free-stream acoustic mode. Nogueira et al. (2022a) confirmed that axisymmetric screech modes can be regarded as an absolute instability associated with the interaction between the downstream-propagating KH waves and upstream-propagating guided jet mode. Furthermore, Nogueira et al. (2022b) found that transition from the A1 to A2 modes is closed by the interaction of the KH mode and the shock system with variations in the spatial wavenumber using absolute instability analysis. This work was extended to rectangular and elliptical jets, showing that their modal staging behavior can also be driven by such triadic interaction (Edgington-Mitchell et al. 2022). For rectangular jets, Gojon et al. (2019) and Wu et al. (2020, 2022) revealed that the screech feedback was closed by the guided jet mode more effectively than by the free-stream acoustic mode.

The addition of an extra jet adds complexity in studying the screech closure mechanism. Whereas a single jet admits self-excited resonance only, twin systems introduce external acoustic waves originating from one jet, completing the self-excitation screech feedback of its pair. Arriving at the receptivity point of its twin with a phase difference consistent with a natural coupling mode between the two jets at a given screech frequency can reinforce the other jet's own screech feedback. In many cases screech tones produced by twin jets are reported to be intermittent, constantly modifying their coupling mode in time for both axisymmetric and rectangular jets (Bell et al. 2021; Karnam et al. 2021; Jeun et al. 2022). Another difficulty arising in twin-jet systems lies in modelling their coupling mode.

In rectangular jets there exists a preferential flapping mode in the minor axis, which somewhat simplifies the modelling work for coupling modes in them. In this paper, we consider the twin version of such rectangular jets, which presents the antisymmetric flapping mode in the minor axis but the symmetric coupling in the major axis at the fundamental screech frequency. Screech tones in this twin system are also intermittent, but the near-field noise data can be divided into several pieces in time that manifest steady antisymmetric coupling for a sufficiently long time to guarantee the frequency resolution

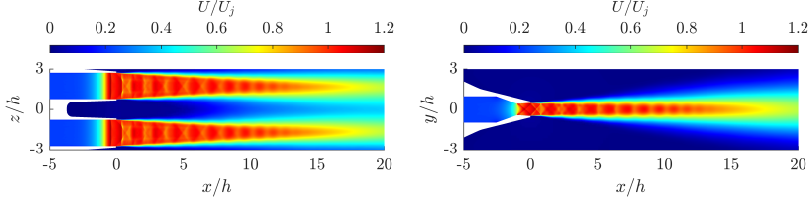


Figure 1: Contours of the time-averaged streamwise velocity normalised by the fully expanded jet velocity (left) in the major axis and (right) in the minor axis.

required for detecting sharp screech tones. An ensemble average of spectral proper orthogonal decomposition (SPOD) modes (Towne et al. 2018) from the resulting segments is then decomposed by the streamwise Fourier transform, to isolate each acoustic wave component of the screech feedback loop. By computing spatial cross-correlation of the decomposed acoustic waves, we aim to discuss which feedback paths dominate the closure mechanism for the rectangular twin-jet screech coupling. To the best of our knowledge, the present study is the first to investigate the nature of the upstream-travelling waves that close the rectangular twin-jet screech coupling, hoping that it can aid to develop a unifying explanation for the jet screech in complex interacting jets.

2. Large-eddy simulation database

In this work we utilize high-fidelity large-eddy simulation (LES) data for jets issuing from twin rectangular nozzles with an aspect ratio of 2 (Jeun et al. 2022), which were computed by a fully compressible unstructured flow solver, charLES, developed by Cascade Technologies (Bres et al. 2017). The twin nozzle had a sharp converging-diverging throat, from which internal oblique shocks formed, and a design Mach number $M_d = 1.5$. The two nozzles were placed closely to each other with the nozzle center-to-center spacing of $3.5h$, mimicking military-style aircraft. Aeroacoustic coupling between the twin jets thus becomes quite important for this flow configuration. The system was scaled by the nozzle exit height h with respect to the origin chosen at the middle of the nozzle exits. The coordinate system was chosen so that the $+x$ axis was defined along the streamwise direction, while y and z axes were defined along the minor and major axis directions of the nozzle at the exit, respectively. The total simulation duration was 1,400 acoustic times (h/c_∞ where c_∞ is the ambient speed of sound).

The LES database was systematically validated against the experiments at various operating conditions. Among the three cases simulated, the present work considers overexpanded twin jets at $\text{NPR} = 3$, which registered the maximum screech. Figure 1 shows the mean streamwise velocity contours in the major and minor axes. The near-field data used for the present analysis were measured in the minor axis planes extending from 0 to 30 in the streamwise direction and from -5 to 5 in the vertical direction, respectively. In these planes probe points were uniformly distributed in both directions with $\Delta x = \Delta y = 0.05h$. The LES data were collected at every $0.1h/c_\infty$. More details on the flow solver and the LES database can be found in Bres et al. (2017) and Jeun et al. (2022), respectively.

3. Twin-jet screech feedback scenarios

Due to the aeroacoustic coupling, the twin-jet screech feedback loop can be completed in two different ways as schematically described in figure 2. In addition to the upstream waves originating in each jet (self-excitation), external acoustic waves radiating from the other jet (cross-excitation) can also play a role in reinforcing one jet's screech feedback loop.

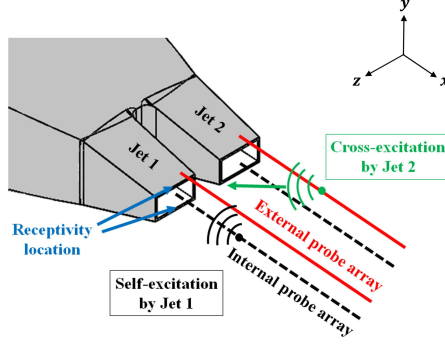


Figure 2: Schematic representation of feedback processes in rectangular twin jets.

Twin-jet coupling is a highly intricate, nonlinear phenomenon, but for simplicity, each self-excitation path is isolated from the other by extracting flow structures in two-dimensional slices in x - y plane at the center of each nozzle in the major axis ($z/h = \pm 1.75$). The dominant flow structures associated with the screech are modelled by the leading SPOD mode at the fundamental screech frequency ($St = 0.37$ where the Strouahl number St is defined based on the equivalent jet diameter and the fully expanded jet velocity U_j). SPOD analysis showed that the SPOD energy spectra of both jets exhibited sharp peaks at the fundamental and second harmonic screech frequencies (Jeun et al. 2022). In particular, at the fundamental screech frequency, the leading SPOD mode contained approximately two orders of magnitudes greater energy than that of the higher-order modes. The relative contribution of the leading mode was measured to be almost 98% of the total energy, justifying the use of the leading SPOD mode.

4. Intermittent screech tones

Time-frequency analysis demonstrated that the screech tones we herein consider are indeed intermittent (Jeun et al. 2022). To investigate why screech tones appear to be irregular in time, the instantaneous phase difference between the two jets is extracted using the Hilbert transform. For a given signal $x(t)$, the Hilbert transform $\tilde{x}(t) = \mathcal{H}[x(t)]$ is computed as

$$\tilde{x}(t) = \mathcal{H}[x(t)] = x(t) \otimes \frac{1}{\pi t}, \quad (4.1)$$

where \otimes denotes the convolution operator. From this, an analytic function of the original signal $\tilde{z}(t)$ can be defined as

$$\tilde{z}(t) = x(t) + i\tilde{x}(t), \quad (4.2)$$

where $i = \sqrt{-1}$. In polar form, (4.2) can be rewritten as

$$\tilde{z}(t) = a(t)\exp[i\theta(t)], \quad (4.3)$$

where

$$\theta(t) = \arctan \left[\frac{\tilde{x}(t)}{x(t)} \right] \quad (4.4)$$

represents the instantaneous phase. Finally, the phase difference between the two jet signals as a function of time is expressed as

$$\Delta\theta(t) = \theta_1(t) - \theta_2(t), \quad (4.5)$$

where the subscripts 1 and 2 represent the jets centered at $z/h = 1.75$ and -1.75 , respectively.

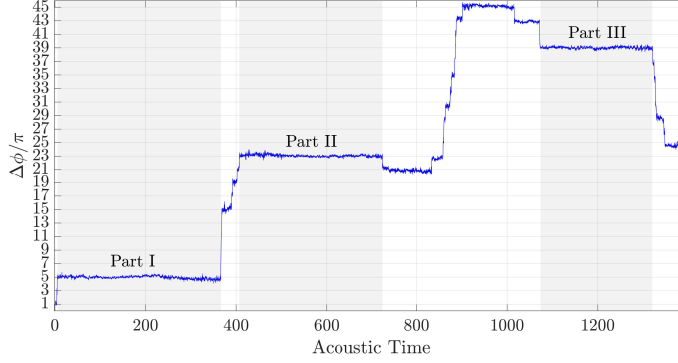


Figure 3: Phase differences between the two jet signals, recovered by the Hilbert transform.

Screech tone of each jet is measured just above the corresponding nozzle exit ($y/h = 1$). The resulting phase difference between the two signals is shown in figure 3 as a function of time. By recalling the scalograms of the corresponding signals (Fig. 24 in Jeun et al. (2022)), one may notice that the phase difference varies aggressively when the change of screech amplitudes is reported in time. Overall, the phase difference represents out-of-phase coupling (odd multiples of π) for a while, followed by a continuous variation between odd and even multiples of π , until it reaches the next plateau of odd multiples. In other words, the interruption of screech tones in our twin rectangular jets seems to be linked to a competition between the antisymmetric and symmetric coupling of the two jets, similarly to the behavior of intermittent tones in underexpanded round twin jets (Bell et al. 2021).

In this regard, complete model for this type of screech feedback loop should be able to include the unsteady phase relationship between the two jets. It is needless to say that constructing such a model is not obvious. As a first step forward, the present work considers a simplified model problem based on the assumption of perfect phase-locking of the twin jets. A way to neglect the effects of intermittency is to select the LES data over periods where the jet-to-jet coupling is perfectly phase-locked only.

5. Analysis of the twin-jet screech feedback loops

5.1. Decomposition of SPOD modes

With the requirement of perfect phase-locking, three different portions of the original LES data, which respectively correspond to the data collected over acoustic time = $[5.5, 366]$, $[407, 725]$, and $[1074, 1320]$ (grey shaded area in figure 3), are selected. To represent flow structures associated with the screech, SPOD analysis is performed onto each partitioned data. Due to the truncation, the frequency resolution for each segment is reduced to $\Delta St = 0.007$. Nevertheless, the length of each partition is still long enough to recover sufficiently narrow screech tones. Depending its length, each partition is split into 2-4 blocks that are windowed by a Hann function with an overlap of 75% to each other such that the length of each realization is given by one-third of the desired number of snapshots that needs to match the experimental frequency resolution. In this way, despite the reduced frequency resolution, SPOD modes can be computed exactly at the (measured) fundamental screech frequency, while still utilizing averaging several realizations for a more accurate estimate and minimised spectral leakage. An ensemble average of the resulting leading SPOD modes is then used to represent wave components constituting the screech feedback.

To extract the upstream and downstream waves in the screech feedback, the SPOD mode is

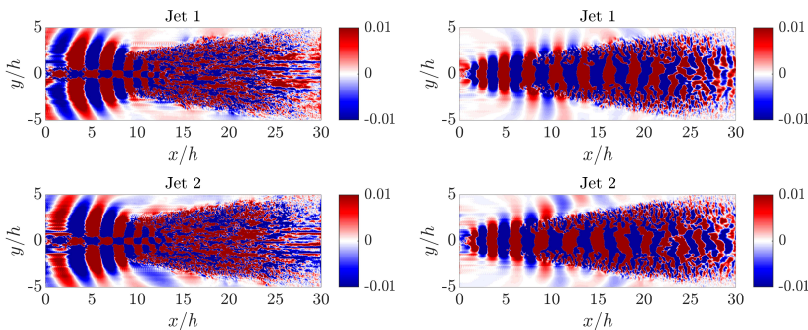


Figure 4: Decomposition of the leading SPOD modes computed by the transverse velocity fluctuations into the (left) upstream- and (right) downstream-propagating components.

decomposed into upstream- and downstream-travelling components based on a wavenumber in x (Edgington-Mitchell et al. 2018; Wu et al. 2020, 2022). Here, the direction of the group velocity of a wave is determined by examining the direction of a phase velocity ($u_p = \omega/k_x$ at a certain frequency ω) as a proxy for it, more specifically, the sign of streamwise wavenumber k_x . Figures 4 visualizes the resulting isolated wave components computed using transverse velocity fluctuations v' . Note that the upstream- and downstream-propagating components show antisymmetric coupling between the two jets at the screech frequency. The upstream-travelling modes include structures confined within the jet and outside of it, which resemble the mode first identified by Tam and Hu (1989). The downstream-propagating modes correspond to the KH instability wavepackets. Throughout this study, we will denote the upstream-propagating guided jet mode by k_- , the upstream-propagating free-stream acoustic mode by c_- , and the downstream-propagating KH mode by k_+ , following the same definition in Wu et al. (2020, 2022).

5.2. Spatial cross-correlation analysis

By following Wu et al. (2020, 2022), for a given zero-mean stationary signal $q(x, y, t)$ a wave detected by two probes placed at different streamwise locations with some time delay τ can be written as

$$q(x_2, y_2, t) = \alpha q(x_1, y_1, t - \tau) + n(t). \quad (5.1)$$

Here, the subscripts represent the two probes, α measures the growth/decay in amplitude, and $n(t)$ is the random noise. Using the auto- and cross-correlation functions, at a given frequency f , one can write the optimal parameters α and τ for a harmonic signal as

$$\tau = -\frac{\arg \zeta}{2\pi f}, \quad \alpha = |\zeta|, \quad \zeta = \frac{\hat{q}_1^* \hat{q}_2}{\hat{q}_1^* \hat{q}_1}, \quad (5.2)$$

where $\hat{q}(f)$ is the Fourier transform of a given signal $q(t)$, and the superscript $*$ denotes the complex conjugate. Screech is an aeroacoustic resonance phenomenon that can be established when a constructive phase relationship is satisfied between the disturbances associated with the feedback loop. Assuming maximum receptivity at the nozzle exit, we seek to identify a downstream streamwise location x where upstream waves originating from such a point arrive at the nozzle exit with an appropriate phase criterion. Mathematically, for the self-excitation path of each jet, such points can be expressed as

$$x \quad \text{s.t.} \quad [\tau_{k_+}(x) - \tau_-(x)]/T_{sc} = \tau_t/T_{sc} = N, \quad (5.3)$$

where τ_- is the negative time delay, which is either τ_{k_-} or τ_{c_-} depending on the choice of the guided jet mode or the external mode as a closure mechanism, τ_t means the total time delay involved in the feedback loop, T_{sc} represents the screech period, and N is a positive integer.

Each self-excited screech feedback can be influenced by disturbances originating from its twin (cross-excitation path). With respect to a given (screech) source location in Jet 1 (x_1), disturbances originating from eligible points of return in Jet 2 (x_2) must satisfy a certain phase relationship at the nozzle exit. Note that this cross-excitation is purely external. Depending on the coupling mode of the twin jets, x_2 can be written as

$$\begin{aligned} x_2 \quad \text{s.t.} \quad \tau_{t,2 \rightarrow 1}/T_{sc} &= [\tau_{k_{+,1}}(x_1) - \tau_{c_{-,2 \rightarrow 1}}(x_2)]/T_{sc} \\ &= \begin{cases} N & \text{(in-phase coupling)} \\ N + \frac{1}{2} & \text{(out-of-phase coupling)} \end{cases} \end{aligned} \quad (5.4)$$

Here, x_1 and x_2 are not necessarily the same. Analogous relationship holds for the cross-excitation by Jet 1 onto Jet 2.

To represent the free-stream acoustic mode (k_+), the upstream-propagating component of the leading SPOD mode computed by pressure fluctuations (p' -SPOD) is taken along $y/h = 5$ with respect to the reference location at $(x/h, y/h) = (0, 0.5)$. In contrast, to consider the upstream-travelling instability waves within the jet plume (k_-) and the KH mode (k_+), the decomposition of the leading SPOD modes computed by transverse velocity fluctuations (v' -SPOD) is taken along $y/h = 0.1$. Finally, the influence onto on jet by the other ($c_{-,2 \rightarrow 1}$ or $c_{-,1 \rightarrow 2}$) is again extracted from the leading p' -SPOD mode.

Figure 5 shows the time delay and the relative amplitude variations of the four different modes associated with the screech coupling with respect to Jet 1. From top to bottom, results are obtained by the $c_{-,1}$, $k_{-,1}$, $k_{+,1}$, and $c_{-,2 \rightarrow 1}$ modes, respectively. Cross-excitation is considered with respect to either the free-stream mode ($c_{-,2 \rightarrow 1|c_{-,1}}$) or the guided jet mode ($c_{-,2 \rightarrow 1|k_{-,1}}$). For each mode, harmonic signals are tracked along the grey solid line as shown in the left columns. Screech feedback loop of Jet 2 reinforced by Jet 1 can likewise be obtained but omitted for simplicity. The strengths of the signals may vary as the probe locations change, but similar outcomes are observed for other transverse probe locations.

As shown in the middle columns the total time delay of each signal changes almost linearly as the probe location moves downstream. The slope represents the phase velocity of it, indicating that the upstream-travelling modes have negative phase velocities. The downstream-travelling KH wave has a positive phase velocity ($u_{p,k+}/U_j = 0.68$), which is close to the typical convection velocity of large-scale eddies in turbulent jets. Here, free-stream acoustic waves additionally take account of the travel distance in the cross-stream directions. Their time delay shows a rapid variation with distance near the nozzle exit due to scattering of sound at the nozzle.

The relative amplitude variations are shown in the right columns of figure 5. For free-stream acoustic modes, they vary as $\sim 1/r$ where r is the distance between the probe location and the reference point, as expected for sound propagation. For each feedback path, the eligible points of return are overlaid from $x/h = 2.5$ to 12.5, to highlight parts of the jets with strong acoustic sources for screech. Points for the *self-excitation* closed by the free-stream *acoustic* mode are represented by red squares on the c_- mode (Closure SA), and those for the *self-excitation* closed by the *guided* jet mode are marked by black circles on the k_- mode (Closure SG). Concerning the *cross-excitation* path, on top of the variations of the amplitudes of the $c_{-,2 \rightarrow 1}$ mode, eligible points of return identified with respect to the self-excitation screech feedback closed by the $c_{-,1}$ mode (Closure CA) and the $k_{-,1}$ mode (Closure CG) are represented by magenta crosses and green triangles, respectively. At this frequency, the KH mode exhibits very large amplitudes around $10 < x/h < 15$. It should be

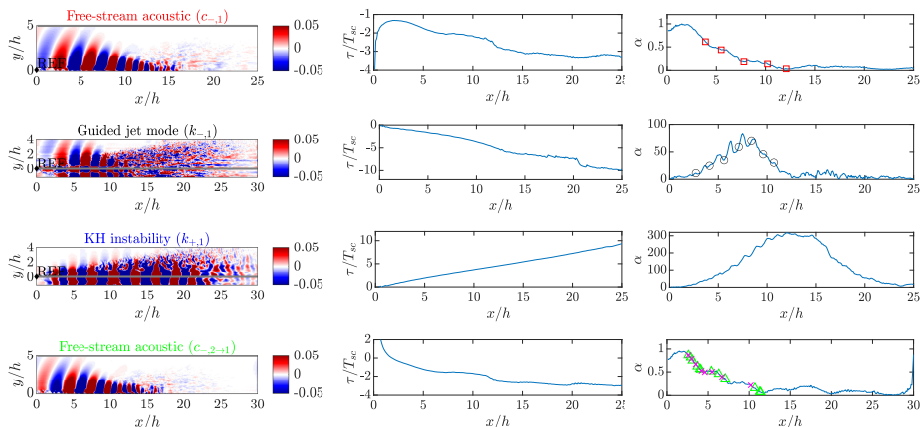


Figure 5: Spatial cross-correlation analysis for the self-excitation by Jet 1 itself and cross-excitation by Jet 2 onto Jet 1 : (left) probe location is denoted by the grey solid line with respect to the reference point marked by the black diamond, (middle) time lag with respect to the reference point, and (right) relative amplitude variation overlaid with the identified points of return represented by symbols: \square , Closure SA; \circ , Closure SG; \times , Closure CA; \triangle , Closure CG.

St	$\max(\alpha_{c-,1})$	$\max(\alpha_{k-,1})$	$\max(\alpha_{k+,1})$	$\max(\alpha_{c-,2 \rightarrow 1 c-,1})$	$\max(\alpha_{c-,2 \rightarrow 1 k-,1})$
0.367	6.10	8.66	61.16	3.01	2.00
0.373	0.61	70.27	317.13	0.86	0.86
0.380	6.32	21.72	109.80	2.49	-

Table 1: Maximum amplitude of each component of the screech feedback loop measured at the screech frequency ($St = 0.373$) and the two neighboring non-resonant frequencies.

also noted that the relative amplitude of the $k_{-,1}$ mode is appreciably larger than that of the $c_{-,1}$ mode. It increases as the probe location moves downstream, peaks around $x/h \approx 7.5$ which corresponds to the 5-6th shock cells, and then decays rapidly farther downstream. Lastly, for the $c_{-,2 \rightarrow 1}$ mode, the CA and CG closure cases show comparable maximum amplitudes.

The fact that compared to the free-stream mode, the guided jet mode shows substantially larger amplitudes indicates that it is more effective in closing the screech feedback. To further examine the dominance of the guided jet mode, similar analyses can be repeated at immediately neighboring, non-resonating frequencies. As shown in table 1, there still exist upstream-propagating guided jet modes at such frequencies, but the amplitudes are much lower than those measured at the screech frequency. In contrast, while the strength of the KH instability decreases dramatically, the relative importance of the free-stream mode becomes greater at these frequencies.

Considering that upstream-travelling waves are driven by interaction of the shock structure and the KH waves, we investigate whether the identified points of return can be related to the locations where such interactions are strong. The strength of shock-instability wave interactions is quantified by the product of the normalised mean transverse velocity V/U_j and the relative amplitude of the KH mode α_{k+} . Each set of the identified points of return are also displayed on top of it, as shown in figure 6. Owing to the two-way symmetry of the rectangular jets in y , the analysis is applied also for the acoustic waves traced along a constant $y < 0$.

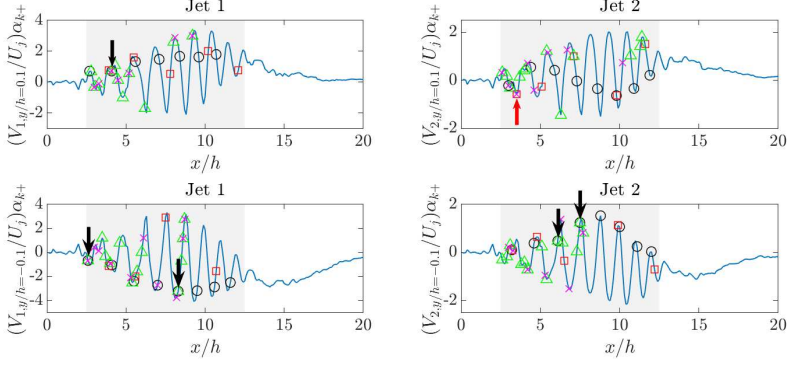


Figure 6: Eligible points of return overlaid on top of $(V_{y/h=\pm 0.1}/U_j)\alpha_{k_+}$: \square , Closure SA; \circ , Closure SG; \times , Closure CA; \triangle , Closure CG. Downward arrows (\downarrow) count the synchronisation of points of return for the Closure CG and SG, while upward arrows (\uparrow) denote the synchronisation of the Closure CA and SA.

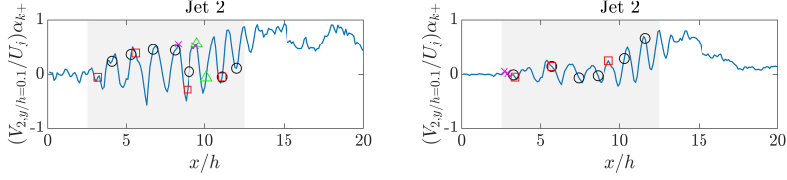


Figure 7: Eligible points of return overlaid on top of $(V_{y/h=0.1}/U_j)\alpha_{k_+}$ at the two immediate neighboring non-resonant frequencies: (left) $St = 0.367$ and (right) $St = 0.383$. Symbols: \square , Closure SA; \circ , Closure SG; \times , Closure CA; \triangle , Closure CG

Figure 6 shows that both the free-stream acoustic mode and the guided jet mode include several eligible points of return. However, for each jet, the guided jet mode (black circles) contains more number of candidates than the free-stream acoustic mode (red squares), and they are mostly located at the peaks of $(V/U_j)\alpha_{k_+}$ curves. Also plotted are the eligible points of return from which the free-stream acoustic waves arrive at the other jet's nozzle lip with an appropriate phase difference (out-of-phase) to reinforce the self-excited screech feedback of that jet. Such points are found with respect to the acoustic waves extracted from both the free-stream acoustic mode (magenta crosses) and the guided jet mode (green triangles). Between the two scenarios, synchronisation with the acoustic source locations for the corresponding self-excitation screech feedback occurs mostly in the case of the guided jet mode (black downward arrows), further confirming the dominant role of this mode in completing the rectangular twin-jet screech.

At the off-peak frequencies, such synchronisation with respect to the guided jet mode rarely happens as shown in figure 7. In this case, weakened guided jet mode hinders each jet's self-excitation as shown in table 1, and the free-stream acoustic waves from its twin fails to reinforce the coupling between the two jets.

6. Conclusions

In this work the effectiveness of the free-stream acoustic mode or the guided jet mode as a closure mechanism for the rectangular twin-jet screech coupling is assessed. Via the isolation of the upstream- and downstream-travelling modes based on the streamwise wavenumber, their spatial cross-correlation determines the phase and amplitude variations of each mode with respect to the receptivity location. Several eligible points of return for each path are

identified, where the upstream-travelling acoustic waves from such points complete the screech feedback loop satisfying the appropriate phase criteria. The present analysis shows that the guided jet mode yields significantly larger amplitudes and admits more number of eligible points of return, which mostly coincide with the peaks of the shock/KH instability waves interaction. Free-stream acoustic waves from such points propagate to the other jet's receptivity location antisymmetrically, reinforcing its self-excited screech feedback loop. At the immediate off-peak frequencies, these observations regarding the gain and phasing are not discernible. The upstream-travelling guided jet mode seems to work as a closure mechanism for the rectangular twin jets as it does for singles jets.

Acknowledgements. The authors acknowledge Cascade Technologies for granting us the access to their numerical software.

Funding. This work was supported by the Office of Naval Research under Grant No. N00014-18-1-2391. Computational resources for LES were provided by the Extreme Science and Engineering Discovery Environment (XSEDE).

Declaration of interests. The authors report no conflict of interest.

REFERENCES

- BELL, G., CLUTS, J., SAMIMY, M., SORIA, J. AND EDGINGTON-MITCHELL, D. 2021 Intermittent modal coupling in screeching underexpanded circular twin jets, *J. Fluid Mech.*, **910** A20.
- BRÈS, G. A., HAM, F. E., NICHOLS, J. W. AND LELE, S. K. 2017 Unstructured large-eddy simulations of supersonic jets, *AIAA J.*, **55** (4), 1164–1184.
- EDGINGTON-MITCHELL, D., JAUNET, V., JORDAN, P., TOWNE, A., SORIA, J. AND HONNERY, D. 2018 Upstream-travelling acoustic jet modes as a closure mechanism for screech, *J. Fluid Mech.*, **855**, R1.
- EDGINGTON-MITCHELL, D., LI, X., LIU, N., HE, F., WONG, T. Y., MACKENZIE, J. AND NOGUEIRA, P. 2022 A unifying theory of jet screech, *J. Fluid Mech.*, **945** A8.
- GOJON, R., BOGEY, C. AND MIHAESCU, M. 2018 Oscillation modes in screeching jets *AIAA J.*, **56** (7), 2918–2924.
- GOJON, R., GUTMARK, E. AND MIHAESCU, M. 2019 Antisymmetric Oscillation Modes in Rectangular Screeching Jets Romain *AIAA J.*, **57** (8), 3422–3441.
- JEUN, J., KARNAM, A., WU, G. J., LELE, S. K., BAIER, F. AND GUTMARK, E. 2022 Aeroacoustics of Twin Rectangular Jets Including Screech: Large-eddy Simulations with Experimental Validation *AIAA J.*, **0** (0), 1–21.
- KARNAM, A., BAIER, F., JEUN, J., WU, G. J. AND LELE, S. K. 2021 An investigation into flow field interactions between twin supersonic rectangular jets *AIAA Paper* 2021-1291.
- LI, X., ZHANG, X., HAO, P. AND HE, F. 2020 Acoustic feedback loops for screech tones of underexpanded free round jets at different modes, *J. Fluid Mech.*, **902**, A17.
- MANCINELLI, M., JAUNET, V., JORDAN, P. AND TOWNE, A. 2019 Screech-tone prediction using upstream-travelling jet modes, *Exp. Fluids*, **60** (1), 22.
- NOGUEIRA, P. A. S., JORDAN, P., JAUNET, V., CAVALIERI, A. V. G., TOWNE, A. AND EDGINGTON-MITCHELL, D. 2022a Absolute instability in shock-containing jets, *J. Fluid Mech.*, **930**, A10.
- NOGUEIRA, P. A. S., JAUNET, V., MANCINELLI, M., JORDAN, P. AND EDGINGTON-MITCHELL, D. 2022b Closure mechanism of the A1 and A2 modes in jet screech, *J. Fluid Mech.*, **936**, A10.
- POWELL, A. 1953 On the mechanism of choked jet noise. *P. Phys. Soc. Lond.* **66**, 1039–1056.
- SHEN, H. AND TAM, C. K. W. 2002 Three-dimensional numerical simulation of the jet screech phenomenon *AIAA J.*, **40** (1), 33–41.
- TAM, C. K. W. AND HU, F. Q. 1989 On the three families of instability waves of high-speed jets *J. Fluid Mech.*, **201**, 447–483.
- TOWNE, A., SCHMIDT, O. T. AND COLONIUS, T. 2018 Spectral proper orthogonal decomposition and its relationship to dynamic mode decomposition and resolvent analysis *J. Fluid Mech.*, **847**, 821–867.
- WU, G. J., LELE, S. K. AND JEUN, J. 2020 Coherence and feedback in supersonic rectangular jet screech In *Annual Research Briefs*, Center for Turbulence Research, Stanford University, 133–144.
- WU, G. J., LELE, S. K. AND JEUN, J. 2022 Analysis of Resonance in Jet Screech with Large-Eddy Simulations *J. Fluid Mech.* (In preparation)